



High macrophage activities are associated with advanced periductal fibrosis in chronic *Opisthorchis viverrini* infection

Journal:	<i>Parasite Immunology</i>
Manuscript ID	Draft
Manuscript Type:	Original Paper
Date Submitted by the Author:	n/a
Complete List of Authors:	Salao, Kanin; Khon Kaen University Faculty of Medicine, Microbiology Watakulsin, Krongkarn; Khon Kaen University Faculty of Medicine, Microbiology Mairiang, Eimorn; Khon Kaen University Faculty of Medicine, Radiology Suttiprapa, Sutas; Khon Kaen University Faculty of Medicine, Academic Affairs Tangkawattana, Sirikachorn; Khon Kaen University Faculty of Veterinary Medicine, Pathobiology Edwards, Steven; University of Liverpool School of Life Sciences, Integrative Biology Sripa, Banchob; Faculty of Medicine, Khon Kaen University, Department of Pathology
Key Words:	Macrophage < Cell, Peripheral blood mononuclear cells < Cell, Human < Host species, Innate immunity < Immunological terms, <i>Opisthorchis viverrini</i> < Parasite, Flow cytometry < Tools and techniques

1
2
3
4 **1 High macrophage activities are associated with advanced periductal fibrosis in chronic**
5
6 **2 *Opisthorchis viverrini* infection**

7
8
9 **3 *Running title:* Innate immunity in opisthorchiasis**
10
11
12 **4**

13 **5 Kanin Salao^{1,7}, Krongkarn Watakulsin^{1,7}, Eimorn Mairiang², Sutas Suttiprapa^{3,7}, Sirikachorn**
14
15 **6 Tangkawattan^{4,7}, Steven W. Edwards⁵, Banchob Sripa^{6,7*}**
16
17
18 **7**

19
20 **8 ¹Department of Microbiology, Faculty of Medicine, Khon Kaen University, Khon Kaen 40002,**
21 **9 THAILAND, Email: kaninsa@kku.ac.th**

22
23
24 **10 ¹Department of Microbiology, Faculty of Medicine, Khon Kaen University, Khon Kaen 40002,**
25 **11 THAILAND, Email: Watakarn@kkumail.com**

26
27 **12 ²Department of Radiology, Faculty of Medicine, Khon Kaen University, Khon Kaen 40002,**
28 **13 THAILAND, Email: eimmai@kku.ac.th**

29
30 **14 ³Tropical Medicine Graduate Program (International Program), Academic Affairs,, Faculty of**
31 **15 Medicine, Khon Kaen University, Khon Kaen 40002, THAILAND, Email: sutasu@kku.ac.th**

32
33 **16 ⁴Department of Pathobiology, Faculty of Veterinary Medicine, Khon Kaen University, Khon**
34 **17 Kaen 40002, THAILAND, Email: sirikach@kku.ac.th**

35
36 **18 ⁵ Institute of Integrative Biology, Faculty of Health and Life Sciences, University of Liverpool,**
37 **19 Liverpool L69 7ZB, UK, Email: S.W.Edwards@liverpool.ac.uk**

38
39 **20 ⁶Department of Pathology, Faculty of Medicine, Khon Kaen University, Khon Kaen 40002,**
40 **21 THAILAND, Email: banchob@kku.ac.th**

41
42 **22 ⁷ WHO Collaborating Centre for Research and Control of Opisthorchiasis (Southeast Asian Liver**
43 **23 Fluke Disease), Tropical Disease Research Center, Faculty of Medicine, Khon Kaen University,**
44 **24 Khon Kaen 40002, THAILAND**

45
46
47 **25**
48
49
50
51 **26 * Corresponding author: Dr.Banchob Sripa, Tropical Disease Research Center (TDRC),**
52 **27 Department of Pathology, Faculty of Medicine, Khon Kaen University, Khon Kaen 40002,**
53
54

1
2
3
4 28 Thailand. Tel: 66-43-363113, Fax: 66-43-204359, E-mail: banchob@kku.ac.th
5
6 29
7
8
9
10
11
12
13
14
15
16
17
18
19
20
21
22
23
24
25
26
27
28
29
30
31
32
33
34
35
36
37
38
39
40
41
42
43
44
45
46
47
48
49
50
51
52
53
54
55
56
57
58
59
60

Abstract

Liver fluke infection caused by *Opisthorchis viverrini* induces several hepatobiliary conditions including advanced periductal fibrosis (APF) and cholangiocarcinoma (CCA), but >25% of the infected population develops APF and 1% develop CCA. The innate immune response is the first line of defense, and macrophages are critical regulators of fibrosis. We hypothesized that macrophages from infected individuals have different capacities to either promote or suppress periductal fibrosis. We compared phagocytic activities of macrophages of healthy individuals and *O. viverrini*-infected individuals \pm APF, and found that macrophages from infected individuals with APF ingested significantly higher numbers of beads compared with healthy controls and *O. viverrini*-infected individuals without APF. To further investigate proteolytic activity, we monitored real-time phagosomal proteolysis of beads conjugated to DQ BODIPY-BSA using live-cell imaging. We show that macrophages from *O. viverrini*-infected individuals with APF also have elevated phagosomal proteolysis activity, which is consistent with their increased phagocytic activity. Additionally, stimulated ROS production by blood monocytes was higher in individuals with APF compared with healthy controls and infected individuals without APF. These results suggest that during *O. viverrini* infection, macrophages with high phagocytic and proteolytic activities together with elevated ROS production, are the phenotypes that can promote tissue damage, which results in periductal fibrosis.

Keywords: *Opisthorchis viverrini*; Innate immunity; Peripheral blood mononuclear cells, Macrophages; Human; Flow cytometry

1
2
3
4 525 6
7 53 **1. INTRODUCTION**

8
9 54 *Opisthorchis viverrini* infection is endemic in the Lower Mekong regions of Southeast Asia,
10
11 55 including Thailand, with approximately 8 million people infected, especially in the northeast of
12
13 56 Thailand where consumption of raw freshwater fishes harboring the infective stage of the parasite
14
15 57 is common (1). Infection can cause several disease manifestations of the bile duct including
16
17 58 cholangitis, cholelithiasis, advanced periductal fibrosis (APF) and the most severe complication,
18
19 59 cholangiocarcinoma (CCA) (2-6). APF provides the basis for malignant transformation to CCA.
20
21 60 Fibrosis occurs when tissues are damaged and normal wound healing responses persist or become
22
23 61 dysregulated (7), usually in response to repetitive tissue injury (8) such as chronic *O. viverrini*
24
25 62 infection (5). Repeated tissue damage results from a combination of factors induced by *O.*
26
27 63 *viverrini* such as 1) physical damage induced by feeding, 2) release of products such as reactive
28
29 64 oxygen species from innate immune cells, 3) and *O. viverrini*-induced host inflammation through
30
31 65 both innate and adaptive immunity (9). The latter mechanism, which involves host immune
32
33 66 responses, is well supported by several findings from our group and others, which have
34
35 67 confirmed that chronic *O. viverrini* infection promotes adaptive proinflammatory responses (10,
36
37 68 11), i.e. IL-6 production (11). However, to date, far less is known about *O. viverrini* effects on
38
39 69 innate immunity.

40
41 70 Macrophages provide defense in innate immunity and these innate immune cells are
42
43 71 among the earliest infiltrating cells after acute *O. viverrini* infection (9). Apart from host defense,
44
45 72 macrophages also play a pivotal role in tissue homeostasis and wound repair. In chronic *O.*
46
47 73 *viverrini* infection that usually leads to persistent inflammation, macrophages produce large

1
2
3
4 74 amounts of mediators that are potentially toxic to the parasites but these may also cause bystander
5
6 75 damage to surrounding host tissues. To compensate for this injury, a small subset of macrophages
7
8
9 76 induce tissue repair, which results in the formation of fibrosis or fibrogenesis (12).
10

11 77 We hypothesized that different rates of development of APF may be due to the
12
13 78 consequence of different levels of innate immune responses that vary among individuals. As
14
15 79 macrophages are part of the innate immune system and critical regulators of fibrosis (13), we
16
17
18 80 sought to determine if *O. viverrini*-infected individuals with APF possess active innate immune
19
20 81 responses (e.g. phagocytic, proteolytic activities and ROS production), and hence have a higher
21
22 82 risk of developing APF compared with individuals without APF. Unraveling this association
23
24
25 83 should take us a step closer toward identifying a high-risk group and possibly providing data for
26
27 84 early and effective diagnosis or primary prevention of APF and CCA.
28

29
30 85

31 32 86 **2. MATERIALS AND METHODS**

33 34 87 **2.1 Sample recruitment**

35
36 88 The current study is an analysis of baseline data collected from a community-based, case-control
37
38
39 89 study of risk factors associated with the development of APF using high resolution
40
41 90 ultrasonography, as previously described (14), from ten villages including Bankae, Banbor,
42
43 91 Nongtu, Nonmakum, Saadsomsri, Jikngam, Songplui, Nhonkho, Huahad, and Somhong in
44
45 92 Kalasin province (Thailand). Overall, 332 individuals aged between 20 and 60 years old were
46
47
48 93 recruited into this study. The control group consisted of 102 *O. viverrini*-infected individuals (60
49
50 94 males, 42 females) without APF (APF-), while the case group consisted of 104 *O. viverrini*-
51
52 95 infected individuals (58 males and 46 females) with APF (APF +). A group of healthy donors
53
54

1
2
3
4 96 consisted of 126 *O. viverrini*-negative participants (68 males and 58 females) (Ov-). Written
5
6 97 informed consents were obtained from all participants. This study complied with the standard
7
8 98 good clinical practice (GCP) guideline and was approved by the Ethics Committee of Khon Kaen
9
10 99 University, Khon Kaen, Thailand, reference number HE591185 and HE480528.
11
12
13
14 100

15 16 101 **2.2 Sample size calculation**

17
18 102 A statistical power analysis was performed for sample size estimation based on data from a
19
20 103 published study (14). The effect size in this study was 0.5, which is considered medium by
21
22 104 Cohen's (1988) criteria. With an alpha = 0.05 and power = 0.80, the projected sample size needed
23
24 105 for this effect size (G*Power 3.1 analysis) is approximately n= 51 per group for the simplest
25
26 106 between-group comparison. Thus, our sample size of >100 per group was more than adequate for
27
28 107 the main objective of this study.
29
30
31
32 108

33 34 109 **2.3 Ultrasonography**

35
36 110 A detailed description of the ultrasonography methods used in this study can be found in previous
37
38 111 publications (14, 15). Using a mobile, high-resolution ultrasound (US) machine (GE model
39
40 112 LOGIQ Book XP, GE healthcare, WI), hepatobiliary abnormalities including portal vein radical
41
42 113 echoes, echoes in liver parenchyma, indistinct gallbladder wall, gallbladder size, sludge and
43
44 114 suspected CCA were graded and recorded. Individuals were classified as having “non-advanced
45
46 115 periductal fibrosis” or “APF-” if the US grade was 0 or 1, and “advanced periductal fibrosis” or
47
48 116 “APF+” if the US grade was 2 or 3. Individuals with alcoholic liver disease, which is seen as
49
50 117 fatty liver by US examination, were excluded. Individuals with marked hepatic fibrosis not
51
52
53
54
55
56
57
58
59
60

1
2
3
4 118 related to *O. viverrini* infection (e.g., cirrhosis from HBV or HCV) were also excluded from this
5
6 119 study.
7
8

9 120

11 121 **2.4 Blood collection**

12
13 122 A total of 20 mL of venous blood collected from the participants by venipuncture, 8 mL of which
14
15 123 was collected in sodium heparin sprayed coated tubes (cat# 367871, Becton Dickinson, NJ) and
16
17 124 used for monocyte isolation.
18
19

20 125

22 126 **2.5 Monocyte isolation for subsequent macrophage generation**

23
24
25 127 The monocyte-derived macrophages (MDMs) used in this study were from peripheral blood
26
27 128 monocytes isolated using a double gradient centrifugation method (16). Briefly, 8 mL of blood
28
29 129 was overlaid on top of 6 mL of Ficoll solution (1.077 g/ml)(cat# 17-1440-02, GE Healthcare Life
30
31 130 Sciences, Singapore) in a 15 mL Falcon tube (cat# 352097, Becton Dickinson, NJ) before
32
33 131 centrifuging at 400x g without braking for 45 min at room temperature. The white band of
34
35 132 peripheral blood mononuclear cells (PBMCs) at the interface was collected and washed 3 times
36
37 133 with PBS and resuspended in 9 mL of RPMI-1640 medium (Cat #11875-093, Thermo Fisher
38
39 134 Scientific, CA). For the second density gradient, 9 mL of the RPMI-resuspended PBMCs were
40
41 135 placed on top of 6 mL of Percoll solution (1.131 g/mL) (cat# 28-9038-33, GE Healthcare Life
42
43 136 Sciences, Singapore) in a 15-mL Falcon tube and centrifuged at 550x g without braking for 45
44
45 137 min at room temperature. The band of monocytes at the interface between the two phases was
46
47 138 collected and washed 3 times with PBS. Monocytes were allowed to differentiate into
48
49 139 macrophages by culturing in RPMI medium supplemented with 10% autologous serum on a 35-
50
51
52
53
54

1
2
3
4 140 mm petri dish (cat# CLS430165, Corning Inc., NY) for 7 days. The MDMs were then cultured in
5
6 141 complete medium (RPMI medium containing 100 µg/mL streptomycin (Cat #15140-122, Thermo
7
8 142 Fisher Scientific, CA), 2 mM L-glutamine (Cat #25030-081, Thermo Fisher Scientific, CA), 50
9
10 143 µM 2-mecaptoethanol, and 10% heat-inactivated fetal calf serum (Cat #14190-250, Thermo
11
12 144 Fisher Scientific, CA).
13
14
15

16 145

18 146 **2.7 Preparation of Alexa Fluor 594 dye and bodipy-BSA conjugated silica beads**

19
20 147 The preparation of silica beads was adapted from the protocol described by Yates and Russell
21
22 148 (17). Briefly, 3.0-µm carboxylate-modified silica particles (Cat #PSi-3.0COOH, Kisker Products
23
24 149 for Biotechnologies, Germany) were conjugated with Alexa Fluor 594 Succinimidyl Esters
25
26 150 (mixed isomers) (Alexa594-SE, Cat #A20004, Thermo Fisher Scientific, CA) or DQ green
27
28 151 BODIPY bovine serum albumin (DQ-BODIPY BSA, Cat #D-12050, Thermo Fisher Scientific,
29
30 152 CA). For opsonization, 0.5 mL of silica beads (14 mg/mL) was mixed with 0.5 mL purified goat-
31
32 153 IgG (5 µg/mL) (Cat # I9140, Sigma-Aldrich, MO) and incubated at 37°C in 5% CO₂ for 30 min.
33
34 154 The opsonized silica beads were then washed, and resuspended in PBS at a concentration of 1
35
36 155 mg/mL.
37
38
39
40

41 156

43 157 **2.8 Synchronized phagocytosis**

44
45 158 MDMs that adhered to a 35-mm petri dish were washed 3 times with PBS and resuspended in
46
47 159 complete medium and then placed on ice for 10 min. Five µL (2x10⁶ particles/mL) silica beads
48
49 160 conjugated with red Alexa Fluor 594 fluorescent dye were added to the petri dish containing
50
51 161 adhered MDMs and mixed gently. The MDMs were then incubated on ice for a further 10 min to
52
53
54

1
2
3
4 162 allow the beads to attach to the cell surface. Synchronised phagocytosis was then triggered by
5
6 163 warming the dish to 37 °C.
7
8

9 164

10 11 165 **2.9 Rate of Phagocytosis**

12
13 166 After 60 min of synchronized phagocytosis of the beads by the MDMs at 37°C in a 5% CO₂
14
15 167 incubator, phagocytosis was stopped by 3 washes with PBS before adding 2 mL of 4%
16
17 168 paraformaldehyde (Cat # P6148, Sigma-Aldrich, MO) and incubated at room temperature for 10
18
19 169 min for fixation. The fixed MDMs were then washed 3 times with PBS. Randomized images of a
20
21 170 total of 100 images were captured using scanning modes for red Alexa Fluor 594 fluorescent dye
22
23 171 (excitation 490 nm, emission 594 nm) using BioStation IM/IM-Q software version 2.21 available
24
25 172 from BioStation IM-Q Time Lapse Imaging System (Nikon, Japan). Images were acquired using
26
27 173 a x40 objective with randomized automated acquisition following the manufacturer's
28
29 174 instructions. The phagocytosed beads were manually counted by an investigator blinded to the
30
31 175 group assignment.
32
33
34
35

36 176

37 38 39 177 **2.10 Rate of Proteolysis**

40
41 178 MDMs that adhered to the petri dish after undergoing synchronized phagocytosis were placed
42
43 179 into a 37 °C chamber containing 5% CO₂ on BioStation IM. The fluorescence intensities of green
44
45 180 reporter DQ BODIPY dye (excitation 490 nm, emission 525 nm) were acquired in 60 sec
46
47 181 intervals for 60 min. Approximately 100 cells were analyzed per sample. The fluorescence
48
49 182 intensity was measured using an ImageJ (64-bit) software (NIH, imagej.nih.gov/ij/download/)
50
51
52
53
54
55
56
57
58
59
60

1
2
3
4 183 and plotted against time using Prism 6 (GraphPad Software Inc., CA) for ratiometric data

5
6 184 analysis of intraphagosomal proteolysis.

7
8
9 185

10 11 186 **2.11 Measurement of ROS production**

12
13 187 50 μl of whole blood was incubated \pm GM-CSF (5 ng/mL) in a total volume of 100 μl in

14
15 188 phosphate-buffered saline. After 30 min incubation at 37°C, samples were treated with 5 μM

16
17 189 dihydrorhodamine 123 followed by addition of either 1 μM fMet-Leu-Phe or 0.1 $\mu\text{g/mL}$ PMA for

18
19 190 a further 5- or 15 min, respectively at 37°C. Flow cytometry was used to measure the production

20
21 191 of ROS.

22
23
24
25 192

26 27 193 **2.12 Statistical analysis**

28
29 194 All data were expressed as the mean \pm SEM. Statistical comparisons were performed using the *t*

30
31 195 test between groups. When serial measurements were taken over time, groups were compared

32
33 196 using two-way repeated-measures ANOVA with Bonferroni correction for multiple comparisons.

34
35 197 A *P* value <0.05 was considered statistically significant. All data were analyzed using GraphPad

36
37 198 Prism 6.0 statistical software.

38
39
40
41 199

42 43 200 **3. RESULTS**

44 45 201 **3.1 MDMs from *O. viverrini*-infected individuals with APF had high phagocytic activity.**

46
47 202 MDMs from *O. viverrini*-infected individuals with APF phagocytosed more beads per cell than

48
49 203 MDMs from healthy controls (Figures 1, A-D: 3.50 ± 0.09 vs 1.58 ± 0.87 ; $n=102/\text{group}$ with

50
51 204 >100 cells analyzed per sample, $p=0.01$, unpaired *t* test) and *O. viverrini*-infected individuals

1
2
3
4 205 without APF (Figures 1, A-D: 3.50 ± 0.09 vs 1.48 ± 0.05 ; n=102/group with >100 cells analyzed
5
6 206 per patient, $p < 0.001$, unpaired t test). We then calculated the percentage of macrophages that
7
8 207 phagocytosed the beads and found that the percentage of phagocytic cells was increased in
9
10 208 individuals with OV infection and increased further in APF+ individuals (Figure 1E). These data
11
12 209 provided the first indication of a possible association between macrophages with high phagocytic
13
14 210 activity and the presence of APF in chronic *O. viverrini* infection.
15
16
17
18
19

20 212 **3.2 MDMs from *O. viverrini*-infected individuals with APF had elevated phagosomal** 21 22 **proteolysis.** 23

24
25 214 We then measured the rate of intraphagosomal proteolysis of individual ingested beads, as the
26
27 215 rate of increased fluorescence of individual particles (increased fluorescence per ingested bead)
28
29 216 by fluorescence imaging microscopy. The rate of proteolysis of BSA protein after phagocytosis
30
31 217 (measured by BODIPY fluorescence intensity) by MDMs from *O. viverrini*-infected individuals
32
33 218 with APF (Figure 2C) was greater than that from non-APF individuals (Figure 2B) and healthy
34
35 219 controls (Figure 2A) at 30 min and 60 min after phagocytosis. The time course of BSA
36
37 220 proteolysis clearly indicated that MDMs from patients with *O. viverrini*-induced APF proteolysed
38
39 221 BSA faster than MDMs from the healthy controls (Figure 2D, n=102/group with 10-15 individual
40
41 222 beads measured for each sample, $p < 0.001$, two-way repeated-measures ANOVA) and *O.*
42
43 223 *viverrini*-infected individuals without APF (Figure 2D, $p < 0.001$, two-way repeated-measures
44
45 224 ANOVA).
46
47
48
49
50
51
52
53
54
55
56
57
58
59
60

1
2
3
4 226 **3.3 ROS production is elevated in monocytes from *O. viverrini*-infected individuals with**
5
6 227 **APF.**

7
8
9 228 Because macrophages used in previous two experiments are derived from peripheral blood
10
11 229 monocytes, we then measured the production of ROS from circulating monocytes in these three
12
13 230 cohorts. We found that there were no differences between groups if the cells in unprimed cells
14
15 231 regardless of the stimulants. For example, there were no differences in ROS production in GM-
16
17 232 CSF primed or unprimed cells when stimulated by the protein kinase C activator, PMA (data not
18
19 233 shown). However, significant differences in ROS production were observed in response to the
20
21 234 peptide, fMet-Leu-Phe which activates receptor-mediated stimulation of ROS, particularly after
22
23 235 exposure to priming agents. In the absence of the priming agent, GM-CSF, there were no
24
25 236 differences in ROS production between the three cohorts and fMet-Leu-Phe did not activate ROS
26
27 237 in the absence of GM-CSF (Figure 3A-C). However, monocytes from *O. viverrini*-infected
28
29 238 individuals with APF produced significantly more ROS than healthy control monocytes and
30
31 239 monocytes from *O. viverrini*-infected individuals without APF (Figure 3D). These data suggest
32
33 240 that circulating monocytes from APF+ individual are capable of generated higher levels of ROS
34
35 241 after priming and stimulation.
36
37
38
39
40

41 242

42
43 243 **4. DISCUSSION**

44
45 244 Liver fluke infection has been widely known for more than two decades as a major cause of
46
47 245 several hepatobiliary diseases including APF (4). The immunopathogenesis of APF is well
48
49 246 described and it is partly induced by host adaptive immune responses through interaction of
50
51 247 several immune cells (9) such as T cells (18), B cells (18), cytokines (11) and reactive oxygen
52
53
54

1
2
3
4 248 species (19). However, far less is known about the role of host innate immune responses on APF
5
6 249 generation. Our studies demonstrate for the first time that MDMs from *O. viverrini*-infected
7
8 250 individuals who have APF have high phagocytosis (Figures 1) and high proteolysis activity
9
10 251 (Figure 2) when compared with both non-*O. viverrini*-infected controls and *O. viverrini*-infected
11
12 252 individuals without APF. Furthermore, circulating monocytes from infected individuals with APF
13
14 253 have elevated ability to generate ROS, compared to infected individuals without APF or healthy
15
16 254 controls. This suggests that the presence of APF may associate with the pro-inflammatory
17
18 255 phenotype of MDMs, consistent with several findings from our group and others (11, 14).

19
20
21
22 256 Phagocytosis is one of several ways for uptake of antigen by macrophages (20). This
23
24 257 process involves the vesicular internalization of solid insoluble particles and can subsequently
25
26 258 activate NF- κ B signal transduction to produce pro-inflammatory cytokines and antimicrobial
27
28 259 peptides (21). These pro-inflammatory products are toxic to invading pathogens, but could also
29
30 260 damage host tissues when deregulated, especially in chronic infection/inflammation. Thus,
31
32 261 enhanced phagocytosis found in MDMs from APF+ individuals could result in an excessive
33
34 262 production of pro-inflammatory mediators such as reactive oxygen species. Indeed, we measured
35
36 263 enhanced ROS production by monocytes in whole blood and found that this was significantly
37
38 264 elevated in infected individuals with APF. Reactive oxygen species could damage host tissues
39
40 265 surrounding the bile ducts, which in turn, undergo repair processes, which result in the
41
42 266 development of fibrosis (22). In support of this hypothesis, a previous study showed that a subset
43
44 267 of MDMs promotes fibrogenesis after chronic *O. viverrini*-induced tissue damage (23).

45
46 268 Another possible mechanism by which pro-inflammatory MDMs could lead to more
47
48 269 advanced fibrosis is by elevated proteolytic activity. Proteolysis activity is tightly regulated by a

1
2
3
4 270 number of protease enzymes (24) and phagosomal pH (25) because effective proteolysis
5
6 271 determines the fate of antigens, influencing antigen processing and presentation, which
7
8 272 determines whether an efficient adaptive immune response is generated. As such, the elevated
9
10 273 proteolysis that observed in this study in MDMs of APF+ individuals could induce stronger
11
12 274 adaptive immune responses, which in turn, could promote robust inflammation, resulting in more
13
14 275 severe host tissue damage and repair.
15
16

17
18 276 Chronic infection leads to inflammation and the production of inflammatory mediators
19
20 277 that are toxic to invading pathogens (25). In the case of helminth infection, the helminthes could
21
22 278 modulate host immune responses and switch immune responses from proinflammatory (Th1) to
23
24 279 anti-inflammatory (Th2) responses (26). The key innate immune cells that play a significant role
25
26 280 in this switching are MDMs, which can switch from M1- to M2-like phenotypes that can induce
27
28 281 Th1 and Th2, respectively. Once recruited to chronic inflamed sites in response to local stimuli,
29
30 282 M1 macrophages drive Th1 responses for pathogen clearance, whereas M2 macrophages drive
31
32 283 Th2 responses for tissue remodeling and fibrosis (12). Therefore, in future studies, identification
33
34 284 of MDM subsets from these populations of *O. viverrini* infected individuals will provide a better
35
36 285 understanding of the mechanisms underlying the development of APF.
37
38
39
40

41 286 In conclusion, we measured and compared the phagocytic and proteolytic activities of
42
43 287 MDMs between non-*O. viverrini*-infected control subjects, and *O. viverrini*-infected individuals
44
45 288 with and without APF. [We also showed elevated ROS production in those with APF.](#) We propose
46
47 289 that in the case of chronic *O. viverrini* infection, tissue resident macrophages with high
48
49 290 phagocytic and proteolytic activities are the phenotypes that could damage bile duct epithelial
50
51 291 and surrounding tissues, which results in the development of APF. Excessive production of
52
53
54
55
56
57
58
59
60

1
2
3
4 292 proinflammatory mediators from these macrophages might have effects on the parasites, but
5
6 293 could also lead to excessive injury of surrounding tissue and hence result in extensive periductal
7
8
9 294 fibrosis.

10
11 295
12
13 296
14
15
16 297 **FUNDING**
17
18 298 This work was supported by the Thailand Research Fund (TRF) grant number RTA 5680006, the
19
20 299 Office of Higher Education Commission of Thailand - the Newton Fund Institutional Links -
21
22 300 British Council, and partially from the National Institute of Allergy and Infectious Diseases
23
24 301 (NIAID), NIH, grant number P50AI098639. BS is a TRF Senior Research Scholar.
25
26
27 302

28
29
30 303 **ACKNOWLEDGEMENTS**

31
32 304 We would like to thank John T. Cathey for editing the manuscript via the Publication Clinic
33
34 305 KKU, Thailand. The content is solely the responsibility of the authors and does not necessarily
35
36 306 represent the official views of the TRF, NIAID, OHEC-Newton Fund, or the NIH or the funders.
37
38

39 307 **AUTHOR CONTRIBUTION**

40
41 308 Conceived and design experiments: KS BS. Performed the experiments: KS EM BS. Analysis
42
43 309 and/or data interpretation: KS ST SS BS. Contributed reagents/materials/analysis/technical
44
45 310 expertise tools: EM SS ST SWE BS. Wrote the paper: KS SS ST SWE BS.
46
47 311

48
49 312 **CONFLICT OF INTERESTS STATEMENT**

50
51 313 The authors declare no conflict of interests.
52
53
54
55
56
57
58
59
60

1
2
3
4 314 **REFERENCES**
5

- 6 315 1. Sripa B, Bethony JM, Sithithaworn P et al. Opisthorchiasis and *Opisthorchis*-
7 associated cholangiocarcinoma in Thailand and Laos. *Acta Trop* 2011; 120 Suppl 1:
8 316 S158-168.
9 317
10
11 318 2. Elkins DB, Mairiang E, Sithithaworn P et al. Cross-sectional patterns of hepatobiliary
12 abnormalities and possible precursor conditions of cholangiocarcinoma associated
13 with *Opisthorchis viverrini* infection in humans. *Am J Trop Med Hyg* 1996; 55: 295-
14 319 301.
15 320
16 321
17 322 3. Mairiang E, Chaiyakum J, Chamadol N et al. Ultrasound screening for *Opisthorchis*
18 *viverrini*-associated cholangiocarcinomas: experience in an endemic area. *Asian Pac*
19 323 *J Cancer Prev* 2006; 7: 431-433.
20 324
21 325 4. Mairiang E, Elkins DB, Mairiang P et al. Relationship between intensity of
22 *Opisthorchis viverrini* infection and hepatobiliary disease detected by
23 326 ultrasonography. *J Gastroenterol Hepatol* 1992; 7: 17-21.
24 327
25 328 5. Mairiang E and Mairiang P. Clinical manifestation of opisthorchiasis and treatment.
26 329 *Acta Trop* 2003; 88: 221-227.
27 330
28 331 6. Sripa B, Kaewkes S, Sithithaworn P et al. Liver fluke induces cholangiocarcinoma.
29 332 *PLoS Med* 2007; 4: e201.
30 333
31 334 7. Wynn TA and Ramalingam TR. Mechanisms of fibrosis: therapeutic translation for
32 fibrotic disease. *Nat Med* 2012; 18: 1028-1040.
33 335
34 336 8. Borthwick LA, Wynn TA and Fisher AJ. Cytokine mediated tissue fibrosis. *Biochim*
35 *Biophys Acta* 2013; 1832: 1049-1060.
36
37
38
39
40
41
42
43
44
45
46
47
48
49
50
51
52
53
54
55
56
57
58
59
60

- 1
2
3
4 336 9. Sripa B, Brindley PJ, Mulvenna J et al. The tumorigenic liver fluke *Opisthorchis*
5
6 337 *viverrini*-multiple pathways to cancer. *Trends Parasitol* 2012; 28: 395-407.
7
8
9 338 10. Pinlaor S, Sripa B, Sithithaworn P and Yongvanit P. Hepatobiliary changes, antibody
10
11 339 response, and alteration of liver enzymes in hamsters re-infected with *Opisthorchis*
12
13 340 *viverrini*. *Exp Parasitol* 2004; 108: 32-39.
14
15
16 341 11. Sripa B, Thinkhamrop B, Mairiang E et al. Elevated plasma IL-6 associates with
17
18 342 increased risk of advanced fibrosis and cholangiocarcinoma in individuals infected
19
20 343 by *Opisthorchis viverrini*. *PLoS Negl Trop Dis* 2012; 6: e1654.
21
22
23 344 12. Murray PJ and Wynn TA. Protective and pathogenic functions of macrophage
24
25 345 subsets. *Nat Rev Immunol* 2011; 11: 723-737.
26
27
28 346 13. Weidenbusch M and Anders HJ. Tissue microenvironments define and get reinforced
29
30 347 by macrophage phenotypes in homeostasis or during inflammation, repair and
31
32 348 fibrosis. *J Innate Immun* 2012; 4: 463-477.
33
34
35 349 14. Mairiang E, Laha T, Bethony JM et al. Ultrasonography assessment of hepatobiliary
36
37 350 abnormalities in 3359 subjects with *Opisthorchis viverrini* infection in endemic
38
39 351 areas of Thailand. *Parasitol Int* 2012; 61: 208-211.
40
41
42 352 15. Sripa B, Mairiang E, Thinkhamrop B et al. Advanced periductal fibrosis from
43
44 353 infection with the carcinogenic human liver fluke *Opisthorchis viverrini* correlates
45
46 354 with elevated levels of interleukin-6. *Hepatology* 2009; 50: 1273-1281.
47
48
49 355 16. Menck K, Behme D, Pantke M et al. Isolation of human monocytes by double gradient
50
51 356 centrifugation and their differentiation to macrophages in teflon-coated cell culture
52
53 357 bags. *J Vis Exp* 2014: e51554.
54
55
56
57
58
59
60

- 1
2
3
4 358 17. Yates RM and Russell DG. Phagosome maturation proceeds independently of
5
6 359 stimulation of toll-like receptors 2 and 4. *Immunity*2005; 23: 409-417.
7
8
9 360 18. Wongratanacheewin S, Good MF, Sithithaworn P and Haswell-Elkins MR. Molecular
10
11 361 analysis of T and B cell repertoires in mice immunized with *Opisthorchis viverrini*
12
13 362 antigens. *Int J Parasitol*1991; 21: 719-721.
14
15
16 363 19. Saichua P, Yakovleva A, Kamamia C et al. Levels of 8-oxodG predict hepatobiliary
17
18 364 pathology in *Opisthorchis viverrini* endemic settings in Thailand. *PLoS Negl Trop Dis*
19
20 365 2015; 9: e0003949.
21
22
23 366 20. Stuart LM and Ezekowitz RA. Phagocytosis: elegant complexity. *Immunity*2005; 22:
24
25 367 539-550.
26
27
28 368 21. Kawai T and Akira S. The role of pattern-recognition receptors in innate immunity:
29
30 369 update on Toll-like receptors. *Nat Immunol*2010; 11: 373-384.
31
32
33 370 22. Duffield JS, Lupper M, Thannickal VJ and Wynn TA. Host responses in tissue repair
34
35 371 and fibrosis. *Annu Rev Pathol*2013; 8: 241-276.
36
37 372 23. Bility MT and Sripa B. Chronic *Opisthorchis viverrini* infection and associated
38
39 373 hepatobiliary disease is associated with iron loaded M2-like macrophages. *Korean J*
40
41 374 *Parasitol*2014; 52: 695-699.
42
43
44 375 24. Reiser J, Adair B and Reinheckel T. Specialized roles for cysteine cathepsins in health
45
46 376 and disease. *J Clin Invest*2010; 120: 3421-3431.
47
48
49 377 25. Watts C. The endosome-lysosome pathway and information generation in the
50
51 378 immune system. *Biochim Biophys Acta* 2012; 1824: 14-21.
52
53
54
55
56
57
58
59
60

1
2
3
4
5
6
7
8
9
10
11
12
13
14
15
16
17
18
19
20
21
22
23
24
25
26
27
28
29
30
31
32
33
34
35
36
37
38
39
40
41
42
43
44
45
46
47
48
49
50
51
52
53
54
55
56
57
58
59
60

379 26. Salgame P, Yap GS and Gause WC. Effect of helminth-induced immunity on infections
380 with microbial pathogens. *Nat Immunol* 2013; 14: 1118-1126.

382

1
2
3
4 383 **FIGURE LEGENDS**

5
6
7 384

8
9 385 **FIGURE 1 MDMs from individuals with *O. viverrini*-induced APF phagocytosed more**
10
11 386 **beads.**

12
13 387 Numbers of phagocytosed opsonized silica beads covalently coupled to Alexa Fluor 594 were
14
15 388 manually counted after synchronized phagocytosis for 60 min with MDMs from healthy
16
17 389 individuals (A), *O. viverrini*-infected individual with no APF (B) and *O. viverrini*-infected
18
19 390 individual with APF (C). Average number of phagocytosed beads per cell was calculated by
20
21 391 manual counts (D). The % of phagocytic cells was also calculated (E). Data represents mean \pm
22
23 392 SEM analyzed using the *t* test. * indicates a *p* value of <0.05 , and mean values are of at least 20
24
25 393 individual cells (chosen blinded) for each of the 102 samples in each cohort.
26
27
28

29
30 394

31
32 395 **FIGURE 2 Proteolysis of MDMs from individuals with *O. viverrini*-induced with and**

33
34 396 **without APF and healthy controls.** Live MDMs that had undergone synchronized phagocytosis
35
36 397 of silica beads covalently coupled with DQ-BODIPY BSA were continuously monitored for 60
37
38 398 min using an inverted live cell BioStation IM microscope. Representative images are shown in
39
40 399 Figures A-C. Upper panels are bright-field images while lower panels are fluorescence images.
41
42 400 The time course of proteolytic activity within the phagosome, measured as gain of fluorescence,
43
44 401 is shown in Figure D. Data are mean \pm SEM analyzed using two-way repeated-measures
45
46 402 ANOVA of 10-15 individual beads measured in each of the 102 samples in each cohort. *
47
48 403 indicates a *p* value of <0.05
49
50

51
52
53 404
54
55
56
57
58
59
60

1
2
3
4 4055
6 4067
8
9 **407 Figure 3 ROS production of monocytes in whole blood**10
11
12 408 Whole blood from healthy controls (OV-) or OV-infected individuals without (OV+/APF-) or13
14 409 with advanced periductal fibrosis (OV+/APF+) were incubated in the absence (unprimed) or15
16 410 presence of 5 ng/mL GM-CSF for 30 min. DHR 123 (at 5 μ M) was then added and then primed17
18 411 or unprimed cells were incubated with or without fMet-Leu-Phe for 5 min before analysis by19
20 412 flow cytometry and gating of monocyte responses. Figure 3A-C show mean fluorescent21
22 413 intensities of DHR123 from OV-, OV+/APF-, OV+/APF+ respectively. Figure 3D, () shows23
24 414 fMet-I-Phe responses in unprimed cells, () GM-CSF responses in the absence of fMet-25
26 415 Leu-Phe and () ROS production by fMet-Leu-Phe in GM-CSF cells. N = 51 per group for27
28 416 GM-CSF primed responses. Data represents mean \pm SEM analyzed using the *t* test. * indicates a29
30 417 p value of <0.05.31 418
32
33
34
35
36
37
38
39
40
41
42
43
44
45
46
47
48
49
50
51
52
53
54
55
56
57
58
59
60

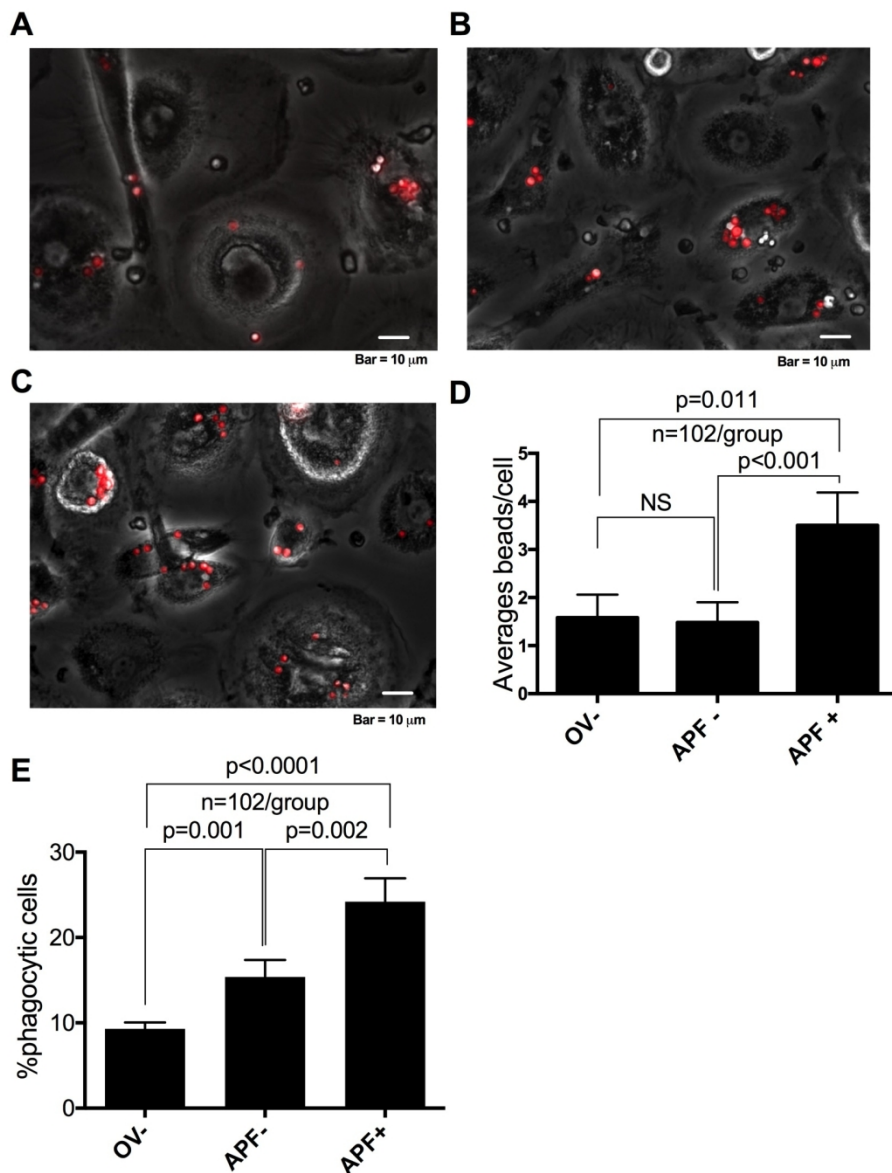


FIGURE 1 MDMs from individuals with *O. viverrini*-induced APF phagocytosed more beads. Numbers of phagocytosed opsonized silica beads covalently coupled to Alexa Fluor 594 were manually counted after synchronized phagocytosis for 60 min with MDMs from healthy individuals (A), *O. viverrini*-infected individual with no APF (B) and *O. viverrini*-infected individual with APF (C). Average number of phagocytosed beads per cell was calculated by manual counts (D). The % of phagocytic cells was also calculated (E). Data represents mean \pm SEM analyzed using the t test. * indicates a p value of <0.05 , and mean values are of at least 20 individual cells (chosen blinded) for each of the 102 samples in each cohort.

142x185mm (300 x 300 DPI)

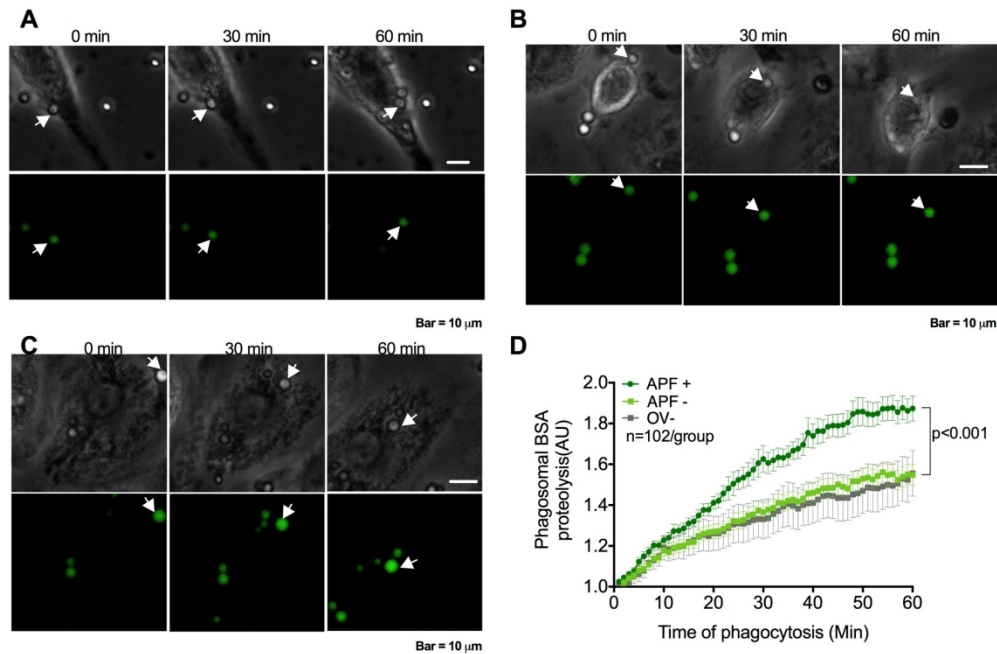


FIGURE 2 Proteolysis of MDMs from individuals with *O. viverrini*-induced with and without APF and healthy controls. Live MDMs that had undergone synchronized phagocytosis of silica beads covalently coupled with DQ-BODIPY BSA were continuously monitored for 60 min using an inverted live cell BioStation IM microscope. Representative images are shown in Figures A-C. Upper panels are bright-field images while lower panels are fluorescence images. The time course of proteolytic activity within the phagosome, measured as gain of fluorescence, is shown in Figure D. Data are mean \pm SEM analyzed using two-way repeated-measures ANOVA of 10-15 individual beads measured in each of the 102 samples in each cohort. * indicates a p value of <0.05

168x113mm (300 x 300 DPI)

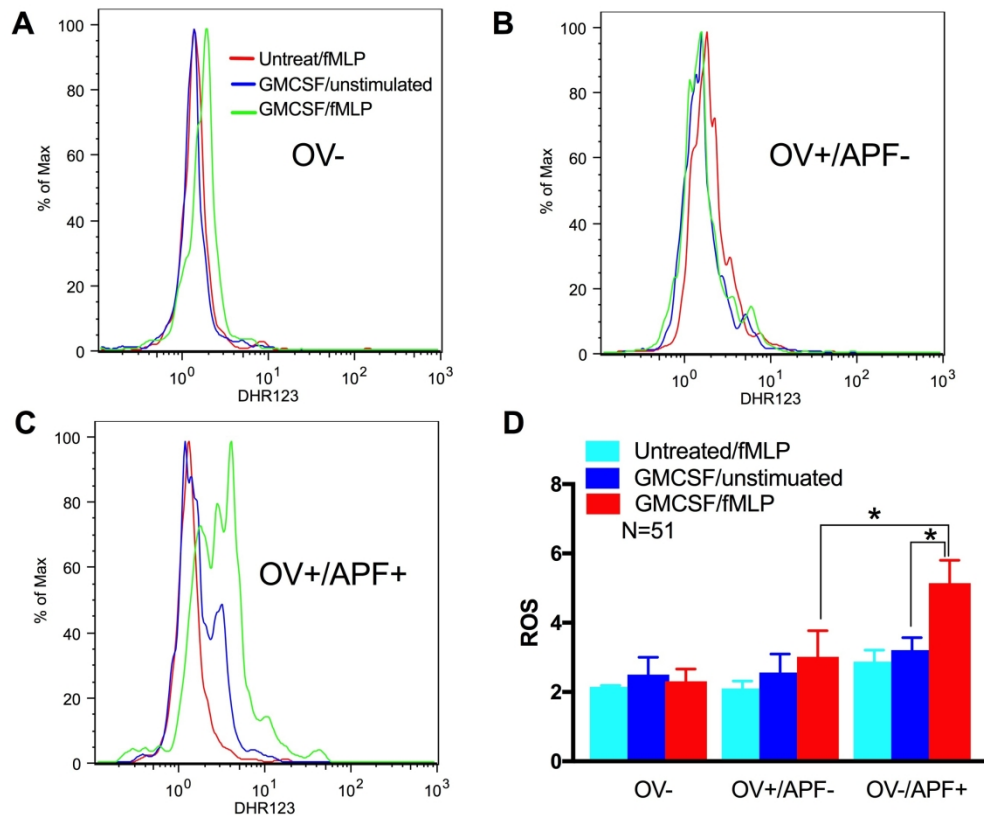


Figure 3 ROS production of monocytes in whole blood

Whole blood from healthy controls (OV-) or OV-infected individuals without (OV+/APF-) or with advanced periductal fibrosis (OV+/APF+) were incubated in the absence (unprimed) or presence of 5 ng/mL GM-CSF for 30 min. DHR 123 (at 5 μ M) was then added and then primed or unprimed cells were incubated with or without fMet-Leu-Phe for 5 min before analysis by flow cytometry and gating of monocyte responses. Figure 3A-C show mean fluorescent intensities of DHR123 from OV-, OV+/APF-, OV+/APF+ respectively. Figure 3D, () shows fMet-Leu-Phe responses in unprimed cells, () GM-CSF responses in the absence of fMet-Leu-Phe and () ROS production by fMet-Leu-Phe in GM-CSF cells. N = 51 per group for GM-CSF primed responses. Data represents mean \pm SEM analyzed using the t test. * indicates a p value of <0.05.

225x186mm (300 x 300 DPI)

Response to reviewers' comments

Reviewer: 1

Comments to the Author

Review on "Association between macrophages phagocytosis activities and advanced periductal fibrosis in chronic opisthorchiasis"

The presented manuscript analyses in vitro generated macrophages (MDM) from patients infected with *O.viverrini* exhibiting (APF+) or free from (APF-) signs of advanced periductal fibrosis. The authors report an enhanced uptake of opsonised silica beads by MDM from APF+ patients. The study seems for the most part technically sound and is well described. However the conclusions drawn seem rather speculative and are only loosely based on the presented data. Overall the extent of the presented findings is very limited and would need further experimental work to corroborate the authors claims.

Response: Thank you for your comments! We agree that the work presented in the previous submission was limited as only phagocytotic and proteolytic assays were included. We have therefore performed more experiments to support our claims and conclusions. We have now measured and compared ROS among these three groups. The results can be found from lines 230-245 and Figure 3.

Individual comments:

The conclusions drawn by the authors seem speculative and one-sided. Phagocytosis per se is not pro-inflammatory but can be anti-inflammatory and prevent chronic inflammation (e.g. phagocytosis of apoptotic cells during cystic fibrosis). Thus, the authors would need to include further data on cytokine production or other inflammatory mediators to clarify whether the enhanced rate of phagocytosis promotes or protects from APF.

Furthermore, the authors repeatedly imply that the altered phagocytosis rate observed in macrophages from APF+ patients may be causative for the formation of fibrosis. However, this is not supported by the presented data. Indeed, since none of the APF- patients (some of whom will develop APF eventually) show altered macrophage phagocytosis it would seem this is a consequence rather than a cause of fibrosis.

Response: In order to address this, we have now performed ROS assays. We found that ROS production by blood monocytes was higher in individuals with APF compared with healthy controls and infected individuals without APF. ROS is a key inflammatory mediator that could cause tissue damage if overexpressed. We believe that elevated ROS production can therefore contribute to tissue damage and promote persistent inflammation. Also, we have re-examined the phagocytosis data and have measured the % of monocytes that underwent phagocytosis (new Figure 1E). This new figure shows that in infected individuals without APF, a greater % of the population of macrophages were capable of phagocytosis, compared to non-infected controls. Therefore, infection *per se* leads to a great phagocytic activity of these macrophages.

1
2
3
4 The data presented in figure 3 is inconclusive and does not reflect on the rate of proteolysis in
5 MDM. If I understand the experimental procedure correctly macrophages were incubated with
6 BSA-Bodipy coupled silica beads and the release of Bodipy measured over time. However, the
7 authors have already shown that MDM from APF+ patients take up more beads in a similar
8 assay. Thus, the increased fluorescent signal might not reflect an altered rate of proteolysis but
9 rather a higher uptake of substrate by the APF+ MDM. Therefore this data cannot be interpreted
10 beyond what has already been shown in figure 1&2 and should be removed. Alternatively the
11 authors would need to provide evidence of substrate normalisation.
12
13

14 Response: This is a very good point raised by the referee but unfortunately, we did not
15 adequately explain the experiment or how the data were obtained. In fact, we actually measured
16 the increase in fluorescence of individual ingested beads. We tracked the release of bodiopy from
17 individual engulfed beads over the first 60 min of phagocytosis, measuring the fluorescence of
18 10-15 individual beads per patient sample (n= 102 patient samples). We apologise for not
19 making the nature of this measurement clear in our first submission. We added a clearer
20 explanation in the manuscript in line 218-220.
21
22
23

24 The flowcytometry data presented in figure 2 and the microscopy pictures shown in figure 1
25 seem to contradict each other. Whereas the microscopy suggests virtually all macrophages do
26 phagocytose opsonised silica beads only about 1% of cells do so according to the flow cytometry
27 data. Is this due to variation in donors and the specific datasets chosen? If so it might be more
28 prudent to chose more representative images / flow-plots.
29

30 Also, please include the flow cytometry data as % positive cells rather than or in addition to the
31 MFI of the whole population.
32
33

34 Response: We agree with these comments. We believe that the phagocytic capacity of the
35 cultured macrophages was grossly perturbed when we scraped them from the culture plates prior
36 to flow cytometry, which explains their very low activity. Therefore, we have removed this
37 figure from the revised manuscript as we believe that the data are not representative of the true
38 phagocytic activity of these cells. The images of phagocytosis shown in Figure 1A-C are single
39 images but we have quantified the number of ingested particles and (new Figure 1E) the number
40 of cultured macrophages (expressed as a % of the total number), that could undergo
41 phagocytosis. We analysed at least 100 cells/patient and believe that these are a truer
42 representation of the phagocytic capacity of these cells.
43
44
45
46

47 Since the authors use autologous serum to generate MDMs in vitro they should include data on
48 the differentiation and activation status (i.e. MHC-expression, costimulatory molecules etc.) of
49 the macrophages from the three groups. Does serum from APF+ patients induce altered
50 differentiation / pre-activation of MDM?
51

52 Response: These are extremely helpful comments, but we now cannot do this retrospectively.
53 We will include such measurements in a new study.
54
55
56
57
58
59
60

1
2
3 Thank you for your invaluable comments.
4
5
6
7

8 **Reviewer: 2**
9

10 Comments to the Author

11 The manuscript entitled "Association between macrophages phagocytosis activities and
12 advanced periductal fibrosis in chronic opisthorchiasis" addresses a major gap in the knowledge
13 on the pathogenesis of chronic opisthorchiasis, namely the role innate immune cells such as
14 macrophages. The authors demonstrate that elevated macrophage phagocytic and proteolytic
15 activities are associated with chronic OV-induced liver fibrosis. This study will establish the
16 basis for more mechanistic studies on the role of macrophages in OV-induced liver disease.
17
18

19 Response: Thank you for your comments!
20
21
22
23
24
25
26
27
28
29
30
31
32
33
34
35
36
37
38
39
40
41
42
43
44
45
46
47
48
49
50
51
52
53
54
55
56
57
58
59
60